Bioresource Technology 277 (2019) 94–103

Contents lists available at ScienceDirect

Bioresource Technology

journal homepage: www.elsevier.com/locate/biortech

Hydrogen and electrical energy co-generation by a cooperative fermentation system comprising *Clostridium* and microbial fuel cell inoculated with port drainage sediment

Vinícius Fabiano dos Passos[a], Rafaella Marcilio[a], Sidney Aquino-Neto[a], Fabrício Butierres Santana[b], Armando Cavalcante Franco Dias[c], Fenando Dini Andreote[c], Adalgisa Rodrigues de Andrade[a], Valeria Reginatto[a,*,1]

[a] Department of Chemistry, Faculty of Philosophy, Sciences and Letters of Ribeirão Preto, University of São Paulo, Ribeirão Preto, SP, Brazil
[b] School of Chemistry and Food, Federal University of Rio Grande, Rio Grande, RS, Brazil
[c] Luiz de Queiroz College of Agriculture - Department of Soil Science, University of São Paulo, Piracicaba, SP, Brazil

ARTICLE INFO

Keywords:
Biohydrogen
Clostridium beijerinckii
MFC
Exolectrogenic culture
Organic acids

ABSTRACT

This research work has succeeded in recovering energy from glucose by generating H_2 with the aid of a *Clostridium beijerinckii* strain and obtaining electrical energy from compounds present in the H_2 fermentation effluent in a microbial fuel cell (MFC) seeded with native port drainage sediment. In the fermentation step, 49.5% of the initial glucose concentration (56 mmol/L) was used to produce 104 mmol/L H_2; 5, 33, 3, and 1 mmol/L acetate, butyrate, lactate, and ethanol also emerged, respectively. MFC tests by feeding the anodic compartment with acetate, butyrate, lactate (individually or as a mixture), or the H_2 fermentation effluent provided power density values ranging between 0.6 and 1.2 W/m^2. Acetate furnished the highest power density with a nanowire-rich biofilm despite the lowest anode bacterial concentration (10^{12} 16S gene copies/g of sediment). Non-conventional exoelectrogenic microbial communities were observed in the acetate-fed MFC; e.g., Pseudomonadaceae (*Pseudomonas)* and Clostridia (*Acidaminobacter*, *Fusibacter*).

1. Introduction

The global energy related to CO_2 emissions has increased considerably in recent years. This has triggered interest in developing new technologies to obtain cleaner fuels from renewable resources. In this context, hydrogen (H_2) appears as an attractive alternative: it is a clean renewable energy source that produces only water after combustion. However, H_2 production on an industrial scale demands high amount of energy and/or fossil fuels (Sinha and Pandey, 2011). In this scenario, H_2 production by dark fermentation (DF) is one of the most environmentally friendly ways to generate H_2 fuel because this process involves mild operating conditions, allows the use of renewable feedstock, and results in biodegradable wastes (Rivera et al., 2017).

Clostridium is the main mesophilic genus of H_2-producing bacteria. These bacteria generate H_2 by carbohydrate fermentation; organic acids, mainly acetic and butyric acids, also emerge as soluble by-products (Eqs. (1) and (2)). The ethanol and lactic acid pathways are less energetic metabolic routes because they do not produce H_2 (Eqs. (3) and (4)) (Sinha and Pandey, 2011).

$$C_6H_{12}O_{6(l)} + 2H_2O_{(l)} \rightarrow 2CH_3COOH_{(l)} + 2CO_{2(g)} + 4H_{2(g)} \quad (1)$$

$$C_6H_{12}O_{6(l)} \rightarrow CH_3CH_2CH_2COOH_{(l)} + 2CO_{2(g)} + 2H_{2(g)} \quad (2)$$

$$C_6H_{12}O_{6(l)} \rightarrow 2CH_3CH_2OH_{(l)} + 2CO_{2(g)} \quad (3)$$

$$C_6H_{12}O_{6(l)} \rightarrow 2CH_3CH(OH)COOH_{(l)} \quad (4)$$

To recover more energy, these byproducts can be further oxidized in different biosystems, such as methane-producing bioreactors, electrolysis cells (which produce more H_2) (Bundhoo, 2017), or Microbial Fuel Cells (MFCs) (which generate electrical energy directly) (Rivera et al., 2017; Sivagurunathan et al., 2017; Yun et al., 2018). Therefore, biotechnologies can be combined to increase energy exploitation of the whole renewable feedstock (Bundhoo, 2017).

MFC has been proposed as an alternative system to produce

* Corresponding author.
E-mail address: valeriars@ffclrp.usp.br (V. Reginatto).
[1] University of São Paulo, Faculty of Philosophy Sciences and Letters of Ribeirão Preto, Department of Chemistry, Av. Bandeirantes 3900, CEP 14040-030, Ribeirão Preto, SP, Brazil.

https://doi.org/10.1016/j.biortech.2019.01.031
Received 12 November 2018; Received in revised form 3 January 2019; Accepted 8 January 2019
Available online 09 January 2019
0960-8524/

electrical energy from effluents, including organic acid-rich effluents from fermentative H_2 production (Pant et al., 2010; Kumar et al., 2016; Sivagurunathan et al., 2017). The use of MFC for this purpose involves organic compound oxidation by microorganisms, which can release extracellular electrons and are therefore called exoelectrogens. Electrons originating from organic material oxidation are transferred to an external circuit, to generate electric current (Logan, 2009).

Combining H_2 production by DF with MFC is interesting because organic acids, like acetate and lactate, are the preferred substrates of exoelectrogens (Pant et al., 2010; Pandey et al., 2016; Khater et al., 2017; Zhang et al., 2017; Estevez-Canales et al., 2018). Moreover, a mixed culture of exoelectrogenic bacteria is advantageous over pure cultures because they involve lower operating costs, dismiss the need for sterilization, are highly adaptable to environmental conditions, and have greater ability to maintain anaerobic conditions through the presence of facultative microorganisms (Zhang et al., 2017). Nevertheless, successful application of the integrated system of H_2 production by DF coupled to energy generation by MFC depends, among other factors, on the stability of the composition of the effluent used to feed the MFC and, consequently, on the stability of the fermentation process (Kumar et al., 2016). Despite the need for sterile conditions, a pure culture of H_2-producing microorganism can provide a more predictable and stable effluent, which could help to improve MFC performance.

Many combinations of biocatalysts can be employed in the integrated systems, but most of them use a mixed culture for DF and in the MFC anode (Bundhoo, 2017; Sivagurunathan et al., 2017). Here, a novel combination of native biocatalysts to harness the glucose energy content is proposed; a *Clostridium beijerinckii* isolate is employed for fermentative H_2 production and a local port drainage sediment is used for electrical energy generation in a MFC

2. Material and methods

2.1. Fermentative H_2 production in batch

C. beijerinckii strain Br21, isolated in our laboratory (Fonseca et al., 2016), was employed in the fermentative H_2 production assays. The fermentation culture medium was modified from P2 through addition of 6.0 g/L yeast extract, 1.0 g/L NaCl, 0.2 g/L $CaCl_2$, and 2.0 g/L NH_4Cl. The described P2 medium consisted of 10 g/L glucose, 1.0 g/L yeast extract, 0.5 g/L K_2HPO_4, 0.5 g/L KH_2PO_4, 0.5 g/L cysteine, 0.4 g/L $MgSO_4{\cdot}7H_2O$, 0.01 g/L $MnSO_4{\cdot}4H_2O$, 0.01 g/L $FeSO_4{\cdot}5H_2O$, 8×10^{-5} g/L biotin, and 0.001 g/L 4-aminobenzoic acid.

C. beijerinckii Br21 pre-inoculum was grown at 35 °C in penicillin-type tubes containing 60 mL of culture medium without oxygen for 24 h. The resulting *Clostridium* pre-inoculum culture was centrifuged at 8981*g* for 5 min and re-suspended in saline solution (0.9% w/v) to adjust the inoculum optical density to 0.1 at 600 nm. Fermentation assays for H_2 production in batch were performed in 100-mL penicillin-type tubes containing 56 mL of culture medium and 4 mL of *Clostridium* inoculum. Argon gas was purged into the tubes for 5 min to ensure air-free atmosphere. The tubes were sealed with a rubber stopper and aluminum seal and incubated at 35 °C for 50 h. pH was manually kept at 5.2 ± 0.3 by adding 0.5 mol/L NaOH dropwise during fermentation. Fermentation assays were carried out in quadruplicate.

Cell, substrate, and product concentrations in the fermentation medium were periodically monitored. Dry cell weight concentration was attained by converting cell culture absorbance at 600 nm into dry cell mass. This correlation has previously been made by relating absorbance at 600 nm with dry suspension mass of different cell culture concentrations. H_2 volume was measured as a function of time with the aid of an inverted flask system containing 5% NaOH (w/v) solution. The inverted flask was coupled to a measuring cylinder, which helped to determine volume variation due to H_2 production. Substrate concentration was measured by high performance liquid chromatography (HPLC) as described below.

2.1.1. Fermentation kinetic parameters

The modified Gompertz model was used to estimate the kinetic parameters of H_2 production in batch. The H_2 volume obtained during the assay as a function of time was treated with the Statistica 7 software and modeled as Equation (5), to obtain R_m, H_{max}, and λ.

$$P = H_{max}.\ \exp\left\{-\exp\left[\frac{R_m.\ e}{P}(\lambda - t) + 1\right]\right\} \quad (5)$$

where P represents the cumulative H_2 volume in assays (mL), H_{max} is the maximum H_2 production potential (mL), R_m indicates the maximum H_2 production rate (mL/h), λ is the lag phase or the time elapsed before H_2 production starts (h), and t is the experiment time (h).

The cell and product yields relative to the substrate consumed in the fermentation assays ($Y_{x/s}$ and $Y_{p/s}$, respectively) were obtained according to Eqs. (6) and (7).

$$Y_{x/s} = \frac{X - X_0}{S_0 - S} \quad (6)$$

$$Y_{p/s} = \frac{P - P_0}{S_0 - S} \quad (7)$$

where X_0 and X are the initial cell concentration and the cell concentration at the end of fermentation (mg/L), respectively; S_0 and S are the substrate concentration at the beginning and end of the assays (mg/L), respectively; and P_0 and P are the product concentration at the beginning and end of fermentation, respectively.

The H_2 volume was converted into mmols by applying the ideal gas equation (Eq. (8)).

$$PV = nRT \quad (8)$$

where P is the atmospheric pressure (1 atm), V is the H_2 volume, n is the number of moles of H_2, R is the ideal gas universal constant (0.082 atm L/K mol), and T is the absolute temperature (K).

2.2. Microbial fuel cell (MFC)

The single-chamber MFC reactor consisted of an anodic compartment coupled with an air-breathing cathode. Briefly, the MFC was constructed by using a 19-mL glass cylinder separated by a gas diffusion membrane (HT1400W, ELAT® GDL–BASF). The MFC contained a 20% platinum cathode (A6 ELAT®) hot pressed with a NAFION® NRE-212 membrane. Hot pressing was carried out at 130 °C and 35 kgf/cm^2 for 180 s. The MFC also contained a carbon cloth (4 cm^2) bioanode that was connected to the potentiostat (EG&G Princeton Applied Research, 273A, USA) by means of a platinum wire (Fig. 1).

Sediment collected from dredging of the Rio Grande port in the State of Rio Grande do Sul, Brazil (coordinates 32°07′S 52°05′W), was employed as MFC anode inoculum. The anodic compartment was filled with 6 mL of sediment containing 19.1 g/L volatile solids and 7 mL of culture medium (1.0 g/L carbon source, 2.5 g/L $NaHCO_3$, 1.9 g/L $Na_2HPO_4{\cdot}12H_2O$, 0.6 g/L $NaH_2PO_4{\cdot}H_2O$, 0.1 g/L $CaCl_2{\cdot}2H_2O$, 0.1 g/L KCl, 1.5 g/L NH_4Cl, 0.1 g/L NaCl, 0.1 g/L $MgCl_2{\cdot}6H_2O$, 0.1 g/L $MgSO_4{\cdot}7H_2O$, 0.005 g/L $MnCl_2{\cdot}4H_2O$, 0.001 g/L $Na_2MoO_4{\cdot}2H_2O$, and 0.05 g/L yeast extract) (Lovley and Phillips, 1988). The following carbon sources were investigated: acetic acid, lactic acid, butyric acid (Sigma-Aldrich, Darmstadt Germany), a synthetic mixture of the three organic acids, and the effluent from *Clostridium* H_2 fermentation, which was employed at the final fermentation concentration.

Before MFC is operated, a stable biofilm must be formed on the anode carbon cloth surface. To this end, the sediment was kept in the anodic compartment for seven days, and a constant current of 165 μA/cm^2 was applied during this period. This current was chosen after preliminary test with the bianode that involved applying different currents in order to determine the current in which maximum potential was attained.

After this start-up phase (seven days), which was also defined after

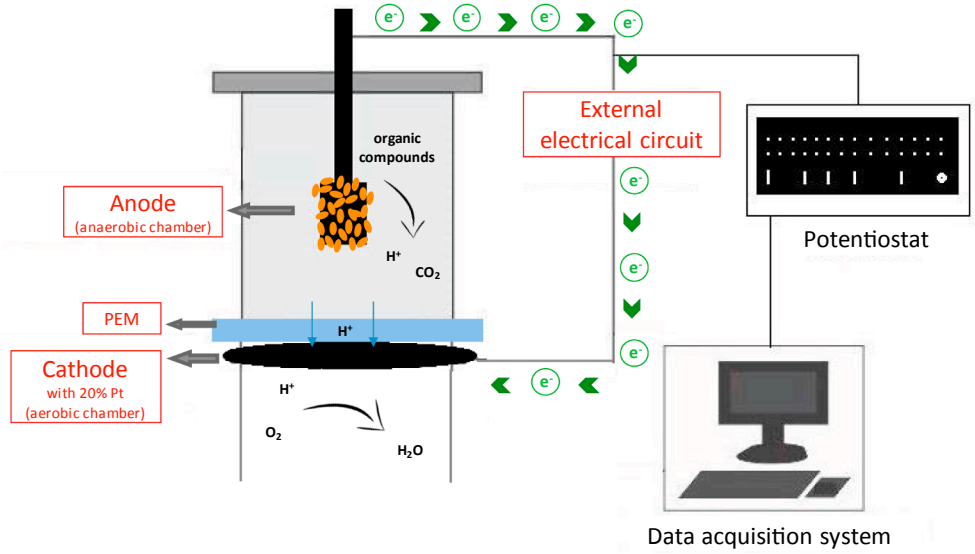

Fig. 1. Setup of the single chamber MFC with open air cathode and its main components.

preliminary tests as the period that was necessary for the biofilm to emerge, the suspended sediment was removed from the anodic compartment, and fresh culture medium was introduced. Argon gas had been purged through the compartment to ensure anaerobiosis during the procedure. The MFC potential was monitored for seven more days under the same applied current density (165 μA/cm^2). A control experiment (FC-control) was accomplished for a similar MFC except for the presence of the microorganism film. The potential value obtained during FC-control was subtracted from the potential value obtained with the MFC operated with organic acid(s) or effluent, which provided the real power density generated by the system after all losses due to resistances from cell operation (Nafion® membrane, cathode, and connections) were subtracted.

2.2.1. Electrochemical parameters

The potential difference (U) generated at the MFC as a function of time at constant current (I) was measured with a potentiostat (EG&G Princeton Applied Research, 273A, USA). These results allowed the MFC power density (P) to be calculated (Eq. (9)).

$$P = \frac{1xU}{A} \tag{9}$$

the units employed in this calculation were W/m^2 (P), Ampere (I), Volt (U), and m^2 (A).

2.3. Energy balance

The amount of energy obtained by fermentation and in the MFC was calculated by Eqs. (10) and (11), respectively.

The amount of energy obtained by glucose conversion into hydrogen is given by:

$$E_{H_2} = \frac{n_{H_2} \times \Delta H_{H_2}}{m} \tag{10}$$

where E_{H2} = energy obtained as hydrogen from degraded glucose as COD-equivalent mass (kJ/gDQO); n_{H2} = number of moles of H_2 produced during the process (mol); ΔH_{H2} = standard enthalpy of hydrogen oxidation (286 kJ/mol); m = glucose mass as COD-equivalent in the fermentation feed (g of COD).

$$E_{MFC} = \frac{i \times V \times \Delta t}{m} \tag{11}$$

where E_{MFC} = energy obtained as electricity from degraded carbon source mass (kJ/g of DQO); i = MFC electric current (0.00066 A); V = voltage during carbon source degradation; Δt = time needed for carbon source degradation (s); m = carbon source as COD-equivalent in the MFC feed (g of COD).

2.4. Analytical determinations

Glucose concentration, as well as acetic acid, lactic acid, butyric acid, and ethanol concentrations in the P2 medium at the beginning and end of fermentation were analyzed by HPLC (LC-20AT, Shimadzu, Japan). The following conditions were used: Aminex column HPX-87H, mobile phase consisting of 0.005 mol/L H_2SO_4, and flow of 0.6 mL/min. Detection was based on refraction index (RID), and data were acquired and treated with the aid of LabSolutions LC/GC 5.85 software (Shimadzu, Japan).

2.5. Statistical analysis

To compare MFC performances, an analysis of variance (ANOVA) and Tukey test at a 5% significance level were accomplished by using the software Statistic 7.0.

2.6. Bioanode microbiological characterization

2.6.1. Scanning electron microscopy (SEM)

A 1-cm^2 anode section was prepared after MFC operation by fixation with 2% (w/v) glutaraldehyde for 3 h and 1% (w/v) osmium tetroxide for 2 h, at 4 °C. The anode biofilm was dehydrated with a water/ethanol gradient and dried until its critical point (Liu and Logan, 2004). The biofilm was coated with gold by sputtering (Bal-Tec, SCD 050, Fürstenstein, Liechtenstein) before being analyzed under a scanning electron microscope (Carl Zeiss, EVO 50, Cambridge, UK).

2.6.2. qPCR analysis

The bacterium was quantified through Quantitative Polymerase Chain Reaction (qPCR) of 16S rRNA. The anodic compartment (inoculum and biofilms after MFC had been operating with a substrate for 14 days) was scraped, washed with PBS buffer 10x, and centrifuged at 8981*g* for 10 min to obtain a cell pellet. The pellet DNA was extracted by using a PowerSoil® DNA Isolation kit (MoBio, Carlsbad, USA), according to the manufacturer's instruction. For sequence analyses, PCR amplification of 16S rRNA gene fragments was performed with primers P1 (5′–CCCTACGGGAGGCAGCAG–3′) and P2 (5′–ATTACCGCGGCTGC

TGG–3′). PCR conditions were the same as the conditions described in the literature (Mosoni et al., 2007). SYBR-Green® Real-Time PCR Mix (Applied Biosystems®) was used as fluorescent label with the aid of StepOne™ Real-Time PCR System (Applied Biosystems®).

To analyze the results, serial dilutions of a 16S rRNA region standard curve were used, which allowed the biofilm sample data to be correlated with curve values. 16S gene copy numbers were achieved per gram of sediment.

2.6.3. 16S rRNA gene sequencing

Microbial community was identified in three samples: native port drainage sediment (inoculum), anode biofilm fed with acetate (MFC-HAc), and anode biofilm fed with H_2 fermentation effluent (MFC-Efflu). 16S rRNA gene sequencing was based on amplification of the V6 region of the bacterium 16S rRNA gene. DNAs extracted from samples were amplified with primers 967F (59-CAACGCGAAGAACCTTACC-39) and 1046R (59-CGACAGCCATGCANCACCT-39). The forward oligonucleotide received distinct markers (identification tags of five base pairs) for each sample. PCR reactions were conducted according to Sogin et al. (2006). Amplification conditions were: final volume of 50 µL containing 5 µL of the first amplification, 1X PCR buffer, 0.2 mM of each oligonucleotide, 0.2 mM of each dNTP, 5 mM $MgCl_2$, 100% BSA, and 0.01 U Taq DNA polymerase (Invitrogen). After amplification, samples were purified with the kit Charge switch PCR Clean-UP (Life Technologies), quantified with 2.0 Qubit Fluorometer (Life Tecnhologies, USA), and sequenced with Ion Torrent Personal Genome Machine three-ion system 316TM chip (Life Technologies, USA), as described by Kavamura et al. (2013). Obtained sequences were compared with sequences published in the NCBI database (National Center for Biotechnology Information).

3. Results and discussion

3.1. Fermentative H_2 production

Fig. 2 shows the H_2 volume generated by *C. beijerinckii* Br21, as well as pH variations during glucose fermentation. Medium pH was adjusted with sodium hydroxide during cell growth to favor substrate consumption and H_2 production. pH values between 5 and 6 favor *Clostridium* growth and H_2 production, thus increasing hydrogenase activity and, consequently, H_2 evolution (Fonseca et al., 2016).

Table 1 lists the Gompertz kinetic parameters obtained during the fermentation assays. The lag phase, the time during which the microorganism leads to the onset of H_2 production, was 13.7 ± 2.6 h. The average maximum H_2 production rate (R_m) was 10.8 ± 1.4 mL/h, and the maximum H_2 volume was 154.4 mL.

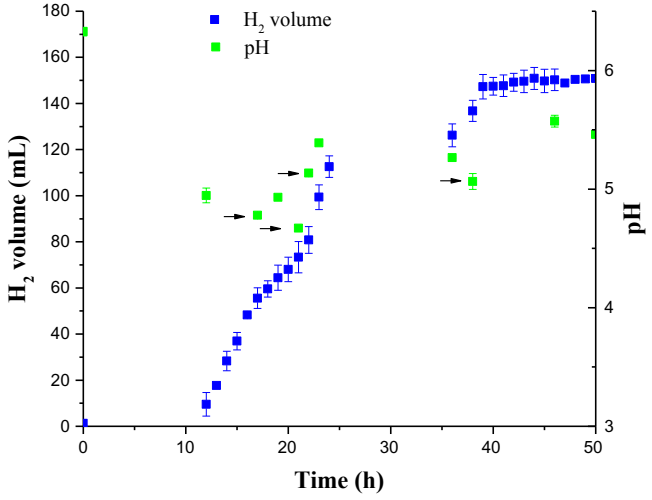

Fig. 2. Generated H_2 volume and pH variation as a function of time during glucose fermentation by *C. beijerinckii* Br21 (→pH adjustment to 5.2 ± 0.3).

Table 1
Kinetic parameters and by-products for H_2 production during fermentative assays in the presence of *C. beijerinckii* Br21.

Kinetic parameter	Average (n = 4)	mmol/L
X_{max} (mg/L)	808.2 ± 25.8	–
Consumed glucose (mg/L)	9590 ± 93	53.3 ± 5.2
ΔpH	0.87 ± 0.02	–
*H_2 (mL)	154.4 ± 7.2	6.11 ± 0.29
*Rm (mL/h)	10.8 ± 1.4	0.43 ± 0.06***
**Butyric acid (mg/L)	2901 ± 435	32.9 ± 4.9
**Acetic acid (mg/L)	300 ± 23	5.0 ± 0.4
**Lactic acid (mg/L)	253 ± 88	2.8 ± 0.9
**Ethanol (mg/L)	44 ± 66	1.0 ± 1.4
$Y_{H2/s}$ mmol of H_2/mmol of glucose	1.98 ± 0.19	
$Y_{x/s}$ mg of X/mmol of glucose	0.08 ± 0.01	
$Y_{a/s}$ mmol of acids/mmol of glucose	0.36 ± 0.02	

* Estimated by fitting of the modified Gompertz model to the experimental data.
** Final concentration in the fermentation effluent.
*** mmol/h.

Substrate conversion to H_2 ($Y_{p/s}$) was 1.98 ± 0.19 mmol of H_2/mmol of consumed glucose (Table 1) and represented about 50% efficiency of substrate conversion into H_2 as compared to the maximum theoretical yield of 4 mmol of H_2/mmol of consumed glucose (Eq. (1)). The H_2 yield resembled the yield described by Fonseca et al. (2016) when they used the same strain but employed galactose as carbon source (2.02 mmol of H_2/mmol of galactose). Masset et al. (2012) obtained 1.45 mmol of H_2/mmol of glucose when they employed a *C. beijerinckii* strain. However, other studies have reported higher yields. For instance, Gomez-Flores et al. (2015) obtained 2.54 mmol of H_2/mmol of substrate during glucose fermentation by a *C. beijerinckii* strain.

Glucose was almost totally consumed at the end of glucose fermentation: only 0.43 g/L glucose remained. Besides high substrate consumption by the bacterial strain, the H_2-producing *C. beijerinckii* Br21 provided a stable effluent composition containing butyrate, acetate, lactate, and low amount of ethanol (Table 1). The butyrate route with lower H_2 conversion (Eq. (2)) represented ca. 80% of the total H_2 production, whereas acetate with higher H_2 conversion ratio (Eq. (1)) corresponded to only 20% (Table 1). Nevertheless, soluble by-products, such as butyric acid, can be further employed as substrate for energy generation at MFC (Sivagurunathan et al., 2017).

3.2. Energy generation at MFC employing organic acid(s) or fermentation effluent as carbon source

Fig. 3 displays the MFC microbial power density obtained after the MFC and the MFC-control power densities were subtracted. Seven days after biofilm growth was established, a very stable power density plot was achieved (Fig. 3). The power generated in the MFC was steady and high irrespective of carbon source even after the MFC had been operated for seven days after a single feed; the power values ranged from 0.5 to 1.25 W/m^2. The power density obtained at the MFC when acetate (MFC-HAc), butyrate (MFC-HBut), lactate (MFC-HLac), acid mixture (MFC-Hmix), or the H_2 fermentation effluent (MFC-Efflu) was used as fuel was 1.2, 0.5, 0.6, 0.7, and 0.6 W/m^2, respectively. When the MFC was fed with the H_2 fermentation effluent (MFC-Efflu), MFC-HBut and MFC-HLac power densities were not significantly different (0.6 –0.7 W/m^2). Butyrate as carbon source (MFC-HBut) gave the lowest power density. However, during MFC-HBut operation, the power output still increased even after 14 days the cell had been fed with butyrate

It is hard to compare MFC data because inoculum, effluent, and MFC configuration can change the overall system efficiency. Schievano et al. (2016), who used two types of integrated systems: anaerobic digestion + single chamber MFC (system 1) and acidogenic

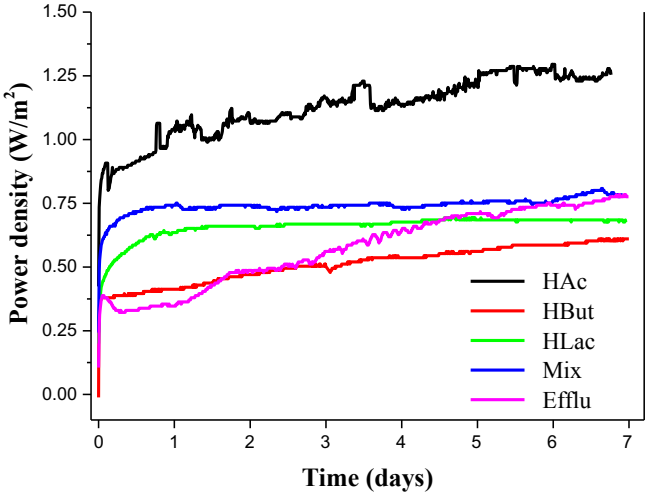

Fig. 3. Power density as a function of time for MFCs fed with different substrates at 1 g/L (HAc = acetic acid; HBut = butyric acid; HLac = lactic acid; Mix = mixture of HAc, HBut, and HLac; and Efflu = fermentation effluent).

fermentation + anaerobic digestion + single chamber MFC (system 2), and who also employed the product of each step as substrate for the next step, described similar power densities, 0.43 and 0.48 W/m^2, respectively.

Increased complexity of the fermentation effluent in relation to acid-containing medium had low effect on MFC performance, except in the case of HAc. The MFC-Efflu power density was similar to the MFC-Mix power density, which was surprising given that the effluent organic load was much higher due to the presence of organic acids and residual glucose from incomplete glucose fermentation. The organic load in MFC-HAc, MFC-HBut, MFC-HLac, MFC-Mix, and MFC-Efflu was 10000, 18132, 10220, 12452, and 36714 g of COD-equivalent/m^{3}d, respectively (Table 2). Organic load and power density output were not correlated, which could be explained by alteration in the carbon source. In general, when the same carbon source is considered, the energy that the system produces increases as the organic content decreases (Elmekawy et al., 2014). Elmekawy et al. (2014) investigated substrate concentrations corresponding to 10, 20, and 30% dilution of the fermentation effluent, which provided organic load of 190, 380, and 570 g of COD/m^{3}d. The lowest load promoted the highest power output, 0.165 W/m^2. Moreover, the reported values were much lower than the values observed here. The highest power density achieved for MFC-HAc (1.25 W/m^2) was much higher than literature data obtained by employing the same substrate (0.09, 0.376, and 0.43 W/m^2, as reported by Khater et al. (2017), Mateo et al. (2018), and Linke et al. (2017), respectively. As stated before, such great differences are probably related to inoculum and MFC configuration.

Butyrate and lactate afforded lower energy recovery in terms of COD mass (kJ/g of COD) as compared to acetate and the acids mixture (Table 2). When the H_2 fermentation effluent was employed to feed MFC-Efflu, energy recovery was similar to MFC-HAc – 13.14 and 14.25 kJ/g of COD, respectively. However, taking the amount of energy from the H_2 fermentation step into account, the integrated system recovered 15.82 kJ/g of COD. Thus, the integrated system represented an improvement of 20% in energy recovery from glucose, compared with MFC-Efflu alone.

Some authors have reported that the integrated system (DF/MFC) improves energy (Table 3). Despite the difficulty in comparing the data because carbon sources, system configurations, and calculations are different, the values obtained from H_2 fermentation and MFC by using the native biocatalysts employed in this work were very promising (Table 3). Sharma and Li (2010) founded 337 J/L as maximum energy recovery in a MFC fed with a H_2 fermentation effluent obtained from a continuous flow mode bioreactor. This value is three times lower than founded here (1052 J/L, Table 3). According to theoretical calculations, 10.42 kJ /L could be recovery in a MFC by employing a dark fermentation effluent from glucose, giving a total of 15.61 kJ /L in an integrated system (Ketheesan and Nirmalakhandan, 2011).

The results endorsed that H_2 fermentation and MFC are an efficient combination not only from the energetic point of view, but also from the environmental standpoint because COD decreases. Glucose transformation into organic acids during fermentation led to only 30% of COD consumption, but it constituted an important step in producing substrates for power generation in MFCs more properly. In the MFC step, acids were consumed, and the total COD removal increased to 92% (Table3).

An acetate-rich fermentation effluent would be more profitable because the MFC-Ac power density was significantly higher as compared to the other MFCs (Table 2). Thus, wild or genetically modified *Clostridium* strains that favor the H_2 acetate route would be more suitable to explore energy in the integrated system (DF/MFC). Although pure cultures can hardly be used under industrial conditions, a pure bacterial isolate with well-known hydrogen-forming activity could be employed because it could lead to bioaugmentation of mixed culture reactors (Kumar et al., 2016). In addition, MFC power densities could be enhanced by improving the bacterial extracellular electron transfer through application of various advanced nanostructured materials like

Table 2
Organic loading, substrate consumption, power density, and energy recovery in MFCs fed with different substrates.

MFC	Organic loading* g of COD/L d	Initial substrate (g/L)	Final substrate (g/L)	Substrate Consumed (g/L)	Substrate Consumed (%)	Voltage (V)	Power Density (W/m^2)	Energy recover kJ/g of COD
HAc	10.1 ± 0.08^a	0.85 ± 0.04^a	0.46 ± 0.01^a	0.39 ± 0.02^a	46 ± 2^a	0.73 ± 0.09^a	1.21 ± 0.16^a	14.25 ± 1.6^a
HBut	18.1 ± 0.53^b	0.91 ± 0.05^a	0.33 ± 0.04^b	0.58 ± 0.04^b	64 ± 4^b	0.30 ± 0.05^b	0.50 ± 0.09^b	3.89 ± 0.32^b
HLac	10.2 ± 0.15^a	0.87 ± 0.04^a	0.15 ± 0.07^c	0.73 ± 0.05^c	84 ± 6^c	0.36 ± 0.02^b	0.64 ± 0.04^b	3.96 ± 0.09^b
Hmix	12.4 ± 0.16^c	0.89 ± 0.06^a	0.32 ± 0.01^b	0.57 ± 0.03^b	64 ± 3^d	0.42 ± 0.01^b	0.74 ± 0.02^c	5.80 ± 0.81^c
HAc	3.4	0.29	0.16	0.13	45			
HBut	5.2	0.26	0.15	0.11	42			
HLac	3.9	0.32	0	0.33	100			
Efflu	36.7 ± 0.3^d	2.85 ± 0.10^b	0.83 ± 0.05^d	1.35 ± 0.07^d	62 ± 3^d	0.36 ± 0.08^b	0.60 ± 0.13^{bc}	13.14 ± 0.93^{ab}
HAc	2.5	0.21	0.17	0.05	24			+
HBut	27.3	1.37	0.66	0.71	52			2.68 ± 0.08**
HLac	1.9	0.16	0	0.16	100			
Glucose	5.0	0.43	0	0.43	100			
								Total = 15.82

Current constant in all experiments at 0.66 mA.
$^{a–d}$Different small caps in the same column indicate significant difference between MFCs, as revealed by Tukey, $p < 0.05$.
* 1g of COD-equivalent (acetic acid = 1.07 g of COD; butyric acid = 1.45 g of COD; lactic acid = 1.07 g of COD; glucose = 1.07 g of COD).
** From H_2 fermentation.

Table 3
Comparison of performances of MFCs fed with H_2-fermentation effluent.

Configuration/Bioanode seed	Effluent feeding MFC	Total COD removal (%)	Maximum Power density (mW/m^2 or W/m^{3*})	Energy recovery	References
Single chamber reactor, working volume of 0.1 L/mixed bacteria	Effluent from H_2 production of domestic wastewater treatment	97	4200*	337 J/L	Sharma and Li (2010)
Dual chambered MFC of 0.03L - cattle manure	Effluent from H_2 production from sucrose	72	165	35.5 kJ/g L d	ElMekawy et al. (2014)
Estimated according theoretical data	Effluent from H_2 production from glucose	90	nc	1042 J/L	Ketheesan and Nirmalakhandan (2011)
Stack MFC two-compartment system with 0.1 L in continuous mode	Effluent from H_2 production from sucrose	82	19.79	nc	Pasupleti et al. (2015)
Single chamber reactor, working volume of 0.013 L marine sediment	Effluent H_2-production from glucose by *C. beijerinckii*	92	600	13.14 kJ/g of COD or 1052 J/L	This work

nc = not calculated.

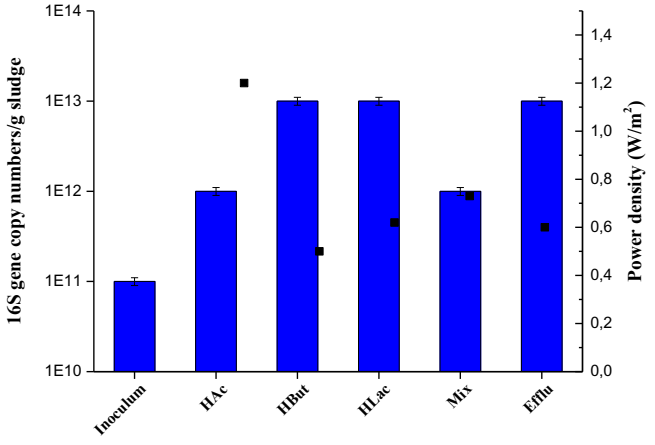

Fig. 4. 16S rRNA gene copy number per gram of sediment in the inoculum and in the MFCs biofilms fed with different substrates and their respective power densities.

nanotubes and graphene, as reviewed by (Kalathil and Pant, 2016).

3.3. Biofilm morphology

Most microorganisms in the biofilm were shaped as rods of varying sizes (data shown in the Supplementary Material only), as described in other works that used a mixed culture from a sewage anaerobic digester (Baranitharan et al., 2015). A mixture of rods and coco-shaped cells has also been verified in MFCs fed with wastewater and soak liquor (Rajeswari et al., 2016). The latter shape was also detected in the MFC-Efflu bioanode, which contained a thicker biofilm. This agreed with the higher 16S RNA concentration in the MFC-Efflu bioanode as compared to the MFC-HAc and MFC-Hmix bioanodes (Fig. 4).

Nanometric structures connecting rod-shaped bacteria were observed in all MFC bioanodes, especially in the MFC-HAc bioanode. These nanostructures were assumed to be nanowires, one of the most important mechanisms of electron transfer by exoelectrogens, such as *Geobacter* spp and *Shewanella onoidensis* (Pirbadian et al., 2014; Estevez-Canales et al., 2018). The prevailing electron transfer mechanism in *Geobacter* spp. takes place with the aid of c-type cytochrome (Estevez-Canales et al., 2018). Alves et al. (2016) reported that cytochromes may form nanowires, which are a new class of proteins found in the genome of several *Geobacter* species and probably account for long-range electron transfer. *Shewanella* species have been described to have nanowires as the main electron extracellular transfer mechanism (Pirbadian et al., 2014).

Although structures for electron transfer emerge, other mechanisms can also rule such transfer. This is especially important in a mixed culture, which can produce molecules that can act as mediators; alternatively, microorganisms can directly perform electron transfer to the electrode (Sacco et al., 2017).

3.4. 16S rRNA gene abundance

qPCR amplification and directed DNA quantification are useful and often employed to measure relative genes copy numbers in a complex DNA and to determine very low microbial community concentrations. Thus, the amplified genes copy number from multiple DNA copies gives the maximum relative microorganism proportion constituting the microbial community. In all MFCs investigated herein, the largest 16S gene copies number relative to the sediment (inoculum) confirmed biofilm growth (Fig. 4). All MFCs presented high biofilm adhesion: about 10^{12}–10^{13} 16S gene copies/g of sediment (Fig. 4). Sotres et al. (2016) reported 10^6 and 10^9 16S gene copies/g of sludge in the MFC anode when they used sludge from sewage and slaughterhouse

treatment plants, respectively.

MFC-HBut, MFC-HLac, and MFC-Efflu (1×10^{13} 16S gene copies/g of sludge) had higher microbial populations than MFC-HAc and MFC-Hmix (1×10^{12} 16S gene copies/g of sediment). Compared to MFC-HLac, MFC-Hmix 16S gene abundance was lower, but its power density was higher (0.62 and 0.73 W/m^2, respectively). Luo et al. (2016) detected high *Shewanella oneidensis* MR-1 abundance in a lactate-fed MFC, which produced 0.19 mA. When the same MFC was fed with lactate and fumarate, the bacterium was able to produce higher electric current (0.29 mA). High butyric acid concentration in MFC-Efflu did not favor power generation probably because the bacterium used this acid for cell growth or transformed it into smaller molecules, such as acetic acid, for further use (Yu et al., 2012).

Because substrate consumption was higher in MFC-Hbut as compared to MFC-HAc, the MFCs did not reach the same power values (Table 2). Thus, although MFC-HBut 16S gene abundance was higher as compared to MFC-HAc, acetate gave the highest power density probably because it provided a more specialized exoelectrogenic biofilm.

3.5. 16S rRNA microbial community gene sequencing

16S rRNA sequencing was conducted to find out which bacterial communities were the most abundant in the sediment (inoculum), in the MFC bioanode that generated the highest energy (MFC-HAc anode), and in the MFC fed with H_2 fermentation effluent (MFC-Efflu anode). The sequences classification were divided by relative abundance of bacterial phylum and classes (Fig. 5A and B, respectively).

As expected, compared to the MFC-HAc and MFC-Efflu bioanodes, the inoculum showed the highest phylum and class variability because it was exposed to uncontrolled environmental conditions. Given the higher phylum variability, the phylum Proteobacteria predominated (more than 50%) in the native port drainage sediment employed as inoculum. Sediments have been successfully employed to seed MFCs because they are rich in microorganisms that can release electrons from organic compound oxidation, which is the case of some genera belonging to the phylum Proteobacteria (Ewing et al., 2017; Xu et al., 2017). Proteobacteria have been reported to prevail in MFC bioanodes, and its abundance is related to higher power output (Ewing et al., 2017). Hence, the native port sediment employed as MFC inoculum proved to be a promising exoelectrogen source.

In the native sediment, the phylum Proteobacteria was well distributed among Gamma-, Delta-, Beta-, and Alpha- proteobacteria with abundances of 12.7, 10.9, 8.3, and 5.5%, respectively (Fig. 5B). However, Proteobacteria had lower dominance in the MFC-HAc and MFC-Efflu bioanodes as compared to inoculum (Fig. 5A). Interestingly, there was two times more and two times less Deltaproteobacteria in the MFC-Efflu (21.1%) and MFC-HAc (4.9%) bioanodes as compared to the sediment (10.9%) (Fig. 5B). Similar results were found when river sediment with high prevalence of the phylum Proteobacteria (53.56%) was used to seed a MFC: its prevalence diminished in the bioanode (from 53.56 to 23.3%), whereas the Deltaproteobacteria fraction increased (7.16% in the sediment and 11.3% in the anode) (Ewing et al., 2017).

Deltaproteobacteria abundance in the MFC-Efflu bioanode (21.1%) confirmed that Deltaproteobacteria participated in electricity generation in this MFC (Table 4). Deltaproteobacteria have been identified as one of the most important bacterial classes in MFCs and underlie direct electron transfer to the electrode. Among Deltaproteobacteria, *Geobacter* spp. is the best-known exoelectrogen and is the genus that is most frequently found in energy generation in acetate-fed MFC (Logan, 2009). According to Estevez-Canales et al. (2018), acetate is the preferred *Geobacter sulfurreducens* electron donor. Karluvali et al. (2015) also reported *Geobacter* as the main genus in bioanodes fed with acetate, but power densities varied between 0.02 and 0.05, which are much lower as compared to the power density found in this work, 1.25 W/m^2. As mentioned above, Deltaproteobacteria abundance in the MFC-HAc anode diminished as compared to the inoculum. *Geobacter* spp. abundance was lower than 0.1% in the MFC-HAc bioanode only, and *Desulfomicrobium* was the most abundant Deltaproteobacteria genus in the MFC-Efflu bioanode (20.1%, Table 4). The genus *Desulfomicrobium* has been described for sulfate-reducing bacteria that do not contain desulfoviridin (a membranous dissimilatory sulfite reductase), and this genus can perform incomplete organic compound oxidation to acetate. *Desulfomicrobium* probably contributed to transforming residual glucose, lactate, ethanol, and butyrate into acetate. *Desulfomicrobium* has frequently been detected in the internal (anaerobic) zones of anode biofilms (Rago et al., 2017).

While Deltaproteobacteria was more abundant in the MFC-Efflu bioanode, Gammaproteobacteria predominated in the MFC-Efflu and MFC-HAc bioanodes, with 29.5 and 39.4%, respectively (Fig. 5B). The most prominent exoelectrogen belonging to the phylum Gammaproteobacteria is *S. onoidensis* MR-1, a facultative anaerobe that frequently occurs in suboxic sediment and soil environments (Jorge and Hazael, 2016). Evidences have pointed to nanowires being the major mechanism for extracellular electron transfer in *S. oneidensis* MR-1, particularly in environments where cells are sessile, including MFC bioanodes (Gorby et al., 2006). S. *oneidensis* MR-1 grows on acetate, but this growth is inhibited at concentrations greater than 10 mM (Tang et al., 2007). At the start of our experiments, acetate concentration in the MFC-HAc bioanode was 16.7 mM, and *Shewanell*a spp. at concentrations higher than 0.1% were not detected in the bioanodes. However, Gammaproteobacteria abundance enhanced in the bioanodes as compared to the inoculum (from 12.7 to 39.4%), indicating that other Gammaproteobacteria consumed acetate and produced energy. In the MFC-HAc and MFC-Efflu bioanodes, the most abundant Gammaproteobacteria families were Pseudomonadacea and Enterobacteriacea at 27.5 and 17.2%, respectively (Table 4). In an activated sludge-seeded MFC, Khater et al. (2017) observed that acetate favored Gammaproteobacteria at 40%, with *Shewanella* spp. and *Pseudomonas* spp. being the most abundant genera. *Pseudomonas* spp. is often described as Gammaproteobacteria involved in electron transfer in MFCs through production of phenazine redox mediators (Bosire et al., 2016).

High Enterobactereacea abundance in the MFC-Efflu bioanode (17.5%) was important for fermentation and/or exogenous electron transfer to the bioanode. Because the MFC-Efflu bioanode had a more diverse substrate spectrum than the MFC-HAc bioanode, it was not surprising that Enterobactereacea abundance was higher in the former bioanode, 17.5 vs 5.4%, respectively. Additionally, some Enterobactereacea, like *Enterobacter cloacae* FR, have broad spectrum of substrate fermentation ability and can generate electricity from glucose, cellulose, lactate, and acetate as a single bacterial strain in a bioanode without exogenous mediators (Rezaei et al, 2009).

Apart from Proteobacteria, Firmicutes also existed in high abundance in the MFC-HAc and MFC-Efflu bioanodes (38.5 and 30.3%, respectively), whereas their abundance in the inoculum was 0.9% (Fig. 5A). Firmicutes have been found in high abundance in some sediments and bioanodes fed with acetate (Khater et al., 2017). Here, the major Firmicutes was Clostridia in both the MFC-HAc and MFC-Efflu bioanodes, 30.8 and 15.7% abundance, respectively (Fig. 5B). Clostridia can use fermentable substrates including lactate to produce acetate, pyruvate, and H_2. Electroactive microorganisms represented by the Deltaproteobacteria group can use the fermentation products as electron donors. This syntrophic association between fermentative bacteria and electroactive microorganisms has been found in many studies in which a fermentable substrate was introduced onto the anode (Ewing et al., 2017). However, the substantial increase in Clostridia abundance on going from the sediment to the MFC-HAc bioanode (0.7 vs 30.8%, respectively) might also be associated with acetate concentration. Tang et al. (2007) observed high Clostridia abundance when they fed a MFC with 1200 mg/L acetate, which was similar to the acetate concentration used here, 850 mg/L. Nevertheless, Clostridia abundance did not rise in a MFC anode seeded with activated sludge acclimated with 150 mg/L of COD as acetate (Park et al, 2017). In the

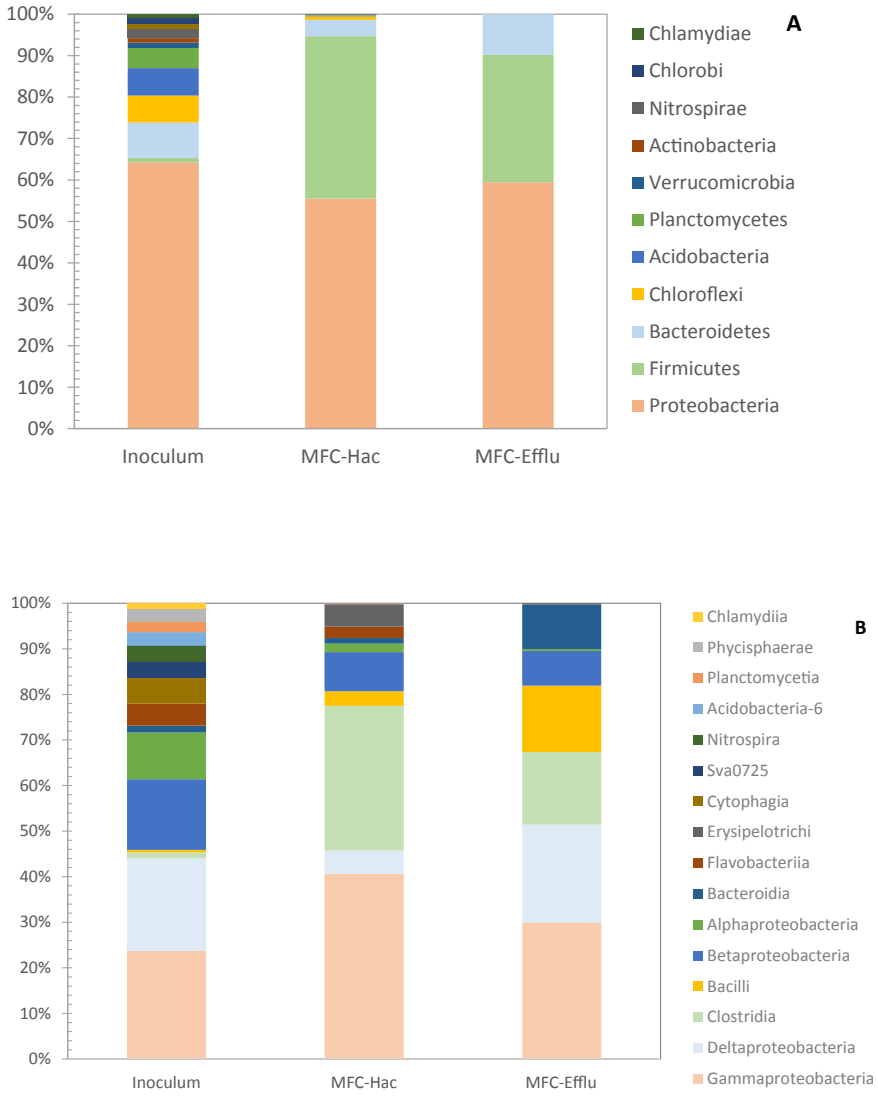

Fig. 5. Relative abundance of sequences based on phylum (A) and class (B) in Inoculum and MFC fed with acetate and effluent as substrate.

MFC-Efflu bioanode, which contained lower acetate concentration, Clostridia abundance was half the Clostridia abundance in the MFC-HAc bioanode, 15.7 and 30.8%, respectively (Fig. 5B). Concerning Clostridia in the MFC-HAc bioanode, *Acidaminobacter* and *Fusibacter* were the most abundant genera, 13.9 and 11.4%, respectively (Table 4). *Acidaminobacter*, which is obligate anaerobe, does not form spores, and does not contain cytochromes, has been isolated from estuarine mud. It can ferment glutamate to give acetate as the major end product together with low amounts of NH_3, formate, CO_2, and H_2. The slow *Acidaminobacter* growth rate can be improved when it is associated with H_2-utilizing bacteria like sulfate-reducing bacteria (Stams and Hansen, 1984). Indeed, the genus *Fusibacter*, which also represented 11.4% of Clostridia in the MFC-HAc bioanode (Table 4), is a fermentative, halotolerant anaerobe with sulfur-reducing features (Fadhlaoui et al., 2015). In the MFC-Efflu bioanode, the most abundant sulfur-reducing bacterium was *Desulfosporosinus*, a genus found in lake sediments and drainage mining sediments. Some species belonging to this genus contain predominantly c-type cytochromes and use lactate as an electron donor to reduce sulfate, sulfite, and thiosulfate (Ramamoorthy et al., 2006). Erysipelotrichacea also had enhanced abundance in the MFC-HAc, but not in the MFC-Efflu bioanode (Table 4). This family has also been observed in great abundance in a bovine and swine sewage-seeded bioanode in air-breathing MFC (Rago et al., 2017).

Bacilli were also detected in both the MFC-Efflu and MFC-HAc MFC bioanodes, at 14.3 and 3.1%, respectively (Fig. 5B). Almost all bacilli in the MFC-Efflu bioanode belong to the family Planococcacea (12%) (Table 4). Planococcacea prevails in soil MFC with higher organic carbon content, but lower pH (Jiang et al, 2016). Indeed the MFC-Efflu bioanode had much higher organic load as compared to the MFC-HAc bioanode, 36,714 and 10,000 g of COD/m^3d, respectively (Table 2).

Thus, substrate type and concentration were the main factors underlying the microbial community composition in MFC bioanodes. In addition, in the acetate-fed MFC, lower microbial diversity correlated with higher cell performance, given that the cell fed with effluent, with greater microbial diversity, did not provide higher power densities.

4. Conclusions

Fermentation coupled with an energy generation system can be very interesting to enhance energy harvesting from organic molecules. The output power density values for the MFCs operating with acetate and H_2-fermentation effluent are very promising as compared to recent literature data. Biofilms with less bacterial growth give higher power density. Acetate is the preferred substrate for energy production, and the high Pseudomonadacea and Clostridiacea (*Acidaminobacter* and *Fusibacter*) abundance in this MFC shows they are important for energy

Table 4
Distribution of the most abundant bacterial classes, families, and genera in the native drainage port sediment (inoculum), MFC-HAc bioanode, and MFC-Efflu bioanode.

Class	Family	Genus	Inoculum (%)	MFC-Hac (%)	MFC-Efflu (%)
Deltaproteobacteria			10.9	4.9	21.1
		Desulfomicrobium	3.4	3	20.1
Gammaproteobacteria			12.7	39.4	29.5
	Enterobacteriacea		0.2	5.4	17.2
	Pseudomonadacea		1.5	27.5	0.4
		Pseudomonas	0.3	5.9	8
Clostridia	Clostridiacea		0.7	30.8	15.7
		Acidaminobacter	0.2	13.9	–
		Clostridium	0.1	0.2	1.8
		Desulfosporosinus	–	–	4.1
		Fusibacter	–	11.4	–
	Peptococcaceae		–	–	4.1
	Ruminococacea		–	1.7	3.8
		Sedimentobacter	–	1.6	1.5
	Erysipelotrichacea		–	4.4	0.3
Bacilli			0.3	3.1	14.3
	Planococcaceae		0.1	–	12
	Exiguobacteracea		–	1.6	–

generation. Enterobacteriacea seems to be involved in energy generation, mainly in the MFC-Efflu bioanode.

Acknowledgements

Financial Support: FAPESP(Fundação de Amparo à Pesquisa do Estado de São Paulo) - Research Grant 2018/00789-7. This study was partly funded by Coordenação de Aperfeiçoamento de Pessoal de Nível Superior - Brasil (CAPES) and Conselho Nacional de Desenvolvimento Científico e Tecnológico (CNPq). V.F.P. received CAPES finance code 001 grants, and R.M received a CNPq grant.

Appendix A. Supplementary data

Supplementary data to this article can be found online at https://doi.org/10.1016/j.biortech.2019.01.031.

References

Alves, M.N., Fernandes, A.P., Salgueiro, C.A., Paquete, C.M., 2016. Unraveling the electron transfer processes of a nanowire protein from *Geobacter sulfurreducens*. Biochim. Biophys. Acta Bioenergy 1857, 7–13.
Baranitharan, E., Khan, M.R., Prasad, D.M.R., Teo, W.F.A., Tan, G.Y.A., Jose, R., 2015. Effect of biofilm formation on the performance of microbial fuel cell for the treatment of palm oil mill effluent. Bioprocess Biosyst. Eng. 38, 15–24.
Bosire, E.M., Blank, L.M., Rosenbaum, M.A., 2016. Strain- and substratedependent redox mediator and electricity production by *Pseudomonas aeruginosa*. Appl. Environ. Microbiol. 82, 5026–5038.
Bundhoo, Z.M.A., 2017. Coupling dark fermentation with biochemical or bioelectrochemical systems for enhanced bio-energy production: a review. Int. J. Hydrogen Energy. 42 (43), 26667–26686.
Elmekawy, A., Srikanth, S., Vanbroekhoven, K., De Wever, H., Pant, D., 2014. Bioelectrocatalytic valorization of dark fermentation effluents by acetate oxidizing bacteria in bioelectrochemical system (BES). J. Power Sources. 262, 183–191.
Estevez-Canales, M., Pinto, D., Coradin, T., Laberty-Robert, C., Esteve-Núñez, A., 2018. Silica immobilization of *Geobacter sulfurreducens* for constructing ready-to-use artificial bioelectrodes. Microb. Biotechnol. 11 (1), 39–49.
Ewing, T., Ha, P.T., Beyenal, H., 2017. Evaluation of long-term performance of sediment microbial fuel cells and the role of natural resources. Appl. Energy 192, 490–497.
Fadhlaoui, K., Ben Hania, W., Postec, A., Fauque, G., Hamdi, M., Ollivier, B., Fardeau, M.L., 2015. *Fusibacter fontis* sp. nov., a sulfur-reducing, anaerobic bacterium isolated from a mesothermic Tunisian spring. Int. J. Syst. Evol. Microbiol. 65 (10), 3501–3506.
Fonseca, B., Guarazzoni, M.E., Reginatto, V., 2016. Fermentative production of H2 from different concentrations of galactose by the new isolate *Clostridium beijerinckii* Br 21. Int. J. Hydrogen Energy 41 (46), 21109–21120.
Gomez-Flores, M., Nakhla, G., Hafez, H., 2015. Microbial kinetics of *Clostridium termitidis* on cellobiose and glucose for biohydrogen production. Biotechnol. Lett. 37, 1965–1971.
Gorby, Y.A., Yanina, S., Mclean, J.S., Rosso, K.M., Moyles, D., Dohnalkova, A., Beveridge, T.J., Chang, I.S., Kim, B.H., Kim, K.S., Culley, D.E., Reed, S.B., Romine, M.F., Saffarini, D.A., Hill, E.A., Shi, L., Elias, D.A., Kennedy, D.W., Pinchuk, G., Watanabe, K., Ishii, S., Logan, B., Nealson, K.H., Fredrickson, J.K., 2006. Electrically conductive bacterial nanowires produced by *Shewanella oneidensis* strain MR-1 and other microorganisms. Proc. Nat. Acad. Sci. 103 (30), 11358–11363.
Jiang, Y.-B., Zhong, W.-H., Han, C., Deng, H., 2016. Characterization of electricity generated by soil in microbial fuel cells and the isolation of soil source exoelectrogenic bacteria. Front. Microbiol. 7, 1776.
Jorge, A.B., Hazael, R., 2016. Use of *Shewanella oneidensis* for energy conversion in microbial fuel cells. Macromol. Chem. Phys. 217 (13), 1431–1438.
Kalathil, S., Pant, D., 2016. Nanotechnology to rescue bacterial bidirectional extracellular electron transfer in bioelectrochemical systems. RSC Adv. 6 (36), 30582–30597.
Karluvali, A., Köroglu, E.O., Manav, N., Çetinkaya, A.Y., Özkaya, B., 2015. Electricity generation from organic fraction of municipal solid wastes in tubular microbial fuel cell. Sep. Purif. Technol. 156, 502–511.
Kavamura, V.N., Taketani, R.G., Lançoni, M.D., Andreote, F.D., Mendes, R., Soares, D.M.I., 2013. Water regime influences bulk soil and Rhizosphere of *Cereus jamacaru* bacterial communities in the Brazilian Caatinga biome. PLoS One 8 (9), e73606.
Ketheesan, B., Nirmalakhandan, N., 2011. Development of a new airlift-driven raceway reactor for algal cultivation. Appl. Energy 88, 3370–3376.
Khater, D.Z., El-Khatib, K.M., Hassan, H.M., 2017. Microbial diversity structure in acetate single chamber microbial fuel cell for electricity generation. J. Genetic Eng. Biotechnol. 15 (1), 127–137.
Kumar, G., Bakonyi, P., Kobayashi, T., Xu, K.Q., Sivagurunathan, P., Kim, S.H., Buitrón, G., Nemestóthy, N., Bélafi-Bakó, K., 2016. Enhancement of biofuel production via microbial augmentation: the case of dark fermentative hydrogen. Renew. Sustain. Energy Rev. 57, 879–891.
Linke, L., Lijuan, Z., Yau Li, S.F., 2017. Evaluation of the performance of zeroelectrolyte-discharge microbial fuel cell based on the type of substrate. RSC Adv. 7, 4070–4077.
Liu, H., Logan, B.E., 2004. Electricity generation using an air-cathode single chamber microbial fuel cell in the presence and absence of a proton exchange membrane. Environ. Sci. Technol. 38, 4040–4046.
Logan, B.E., 2009. Exoelectrogenic bacteria that power microbial fuel cells. Nat. Rev. Microbiol. 7, 375–381.
Lovley, D.R., Phillips, E.J.P., 1988. Novel mode of microbial energy metabolism: organic carbon oxidation coupled to dissimilatory reduction of iron or manganese. Appl. Environ. Microbiol. 54 (6), 1472–1480.
Luo, S., Guo, W., Nealson, K.H., Feng, X., He, Z., 2016. 13C pathway analysis for the role of formate in electricity generation by *Shewanella oneidensis* MR-1 using lactate in Microbial Fuel Cells. Sci. Rep. 6, 1–8.
Masset, J., Calusinska, M., Hamilton, C., Hiligsmann, S., Joris, B., Wilmotte, A., Thonart, P., 2012. Fermentative hydrogen production from glucose and starch using pure strains and artificial co-cultures of *Clostridium* spp. Biotechnol. Biofuels 5 (35), 1–15.
Mateo, S., Cañizares, P., Manuel Andrés, P.R., Francisco Jesus, F.-M., 2018. Driving force behind electrochemical performance of microbial fuel cells fed with different substrates. Chemosphere 207, 313–319.
Mosoni, P., Chaucheyras-Durand, F., Béra-Maillet, C., Forano, E., 2007. Quantification by real-time PCR of cellulolytic bacteria in the rumen of sheep after supplementation of a forage diet with readily fermentable carbohydrates: effect of a yeast additive. J. Appl. Microbiol. 103, 2676–2685.
Pandey, P., Shinde, V.N., Deopurkar, R.L., Kale, S.P., Patil, S.A., Pant, D., 2016. Recent advances in the use of different substrates in microbial fuel cells toward wastewater treatment and simultaneous energy recovery. Appl. Energy 168, 706–723.
Pant, D., Van Bogaert, G., Diels, L., Vanbroekhoven, K., 2010. A review of the substrates used in microbial fuel cells (MFCs) for sustainable energy production. Bioresour. Technol. 101 (6), 1533–1543.
Park, Y., Cho, H., Yu, J., Min, B., Kim, H.S., Kim, B.G., Lee, T., 2017. Response of microbial community structure to pre-acclimation strategies in microbial fuel cells for domestic wastewater treatment. Bioresour. Technol. 233, 176–183.
Pasupleti, S.B., Srikanth, S., Venkata Mohan, S., Pant, D., 2015. Continuous mode operation of microbial fuel cell (MFC) stack with dual gas diffusion cathode design for the treatment of dark fermentation effluent. Int. J. Hydrogen Energy 40 (36), 12424–12435.
Pirbadian, S., Barchinger, S.E., Leung, K.M., Byun, H.S., Jangir, Y., Bouhenni, R.A., Reed, S.B., Romine, M.F., Saffarini, D.A., Shi, L., Gorby, Y.A., Golbeck, J.H., El-Naggar, M.Y., 2014. *Shewanella oneidensis* MR-1 nanowires are outer membrane and periplasmic extensions of the extracellular electron transport components. Proc. Nat. Acad. Sci. 111 (35), 12883–12888.
Rago, L., Cristiani, P., Villa, F., Zecchin, S., Colombo, A., Cavalca, L., Schievano, A., 2017. Influences of dissolved oxygen concentration on biocathodic microbial communities in microbial fuel cells. Bioelectrochemistry 116, 39–51.
Rajeswari, S., Vidhya, S., Krishnaraj, R.N., Saravanan, P., Sundarapandiyan, S., Maruthamuthu, S., Ponmariappan, S., Vijayan, M., 2016. Utilization of soak liquor in microbial fuel cell. Fuel 181, 148–156.
Ramamoorthy, S., Sass, H., Langner, H., Schumann, P., Kroppenstedt, R.M., Spring, S., Overmann, J., Rosenzweig, R.F., 2006. *Desulfosporosinus lacus* sp. nov., a sulfate-educing bacterium isolated from pristine freshwater lake sediments. Int. J. Syst. Evol. Microbiol. 56, 2729–2736.
Rezaei, F., Xing, D., Wagner, R., Regan, J.M., Richard, T.L., Logan, B.E., 2009. Simultaneous cellulose degradation and electricity production by *Enterobacter cloacae* in a microbial fuel cell. Appl. Environ. Microbiol. 75 (11), 3673–3678.
Rivera, I., Bakonyi, P., Cuautle-Marín, M.A., Buitrón, G., 2017. Evaluation of various cheese whey treatment scenarios in single-chamber microbial electrolysis cells for

improved biohydrogen production. Chemosphere 174, 253–259.
Sacco, N.J., Bonetto, M.C., Cortón, E., 2017. Isolation and characterization of a novel electrogenic bacterium, *Dietzia* sp. RNV-4. PLoS One 12 (2), e0169955.
Schievano, A., Sciarria, T.P., Vanbroekhoven, K., Wever, H. De, Puig, S., Andersen, S.J., Rabaey, K., Pant, D., 2016. Electro-fermentation - merging electrochemistry with fermentation in industrial applications. Trends Biotechnol. 34 (11), 866–878.
Sharma, Y., Li, B., 2010. Optimizing energy harvest in wastewater treatment by combining anaerobic hydrogen producing biofermentor (HPB) and microbial fuel cell (MFC). Int. J. Hydrogen Energy 35 (8), 3789–3797.
Sinha, P., Pandey, A., 2011. Na evaluative report and challenges for fermentative biohydrogen production. Int. J. Hydrogen Energy 36 (13), 7460–7478.
Sivagurunathan, P., Kuppam, C., Mudhoo, A., Saratale, G.D., Kadier, A., Zhen, G., Chatellard, L., Trably, E., Kumar, G., 2017. A comprehensive review on two-stage integrative schemes for the valorization of dark fermentative effluents. Crit. Rev. Biotechnol. 38 (6), 868–882.
Sogin, M.L., Morrison, H.G., Huber, J., Welch, M.D., Huse, S.M., Neal, P.R., Neal, P.R., Arrieta, J.M., Herndl, G.J., 2006. Microbial diversity in the deep sea and the underexplored "rare biosphere". Proc. Natl. Acad. Sci. 103 (32), 12115–12120.
Sotres, A., Cerrillo, M., Viñas, M., Bonmatí, A., 2016. Nitrogen removal in a two-chambered microbial fuel cell: establishment of a nitrifying-denitrifying microbial community on an intermittent aerated cathode. Chem. Eng. J. 284, 905–916.
Stams, A.J.M., Hansen, T.A., 1984. Fermentation of glutamate and other compounds by *Acidaminobacter hydrogenoformans* gen. nov. sp. nov., an obligate anaerobe isolated from black mud. Studies with pure cultures and mixed cultures with sulfate-reducing and methanogenic bacteria. Arch. Microbiol. 137 (4), 329–337.
Tang, Y.J., Meadows, A.L., Keasling, J.D., 2007. A kinetic model describing *Shewanella oneidensis* MR-1 growth, substrate consumption, and product secretion. Biotechnol. Bioeng. 96 (1), 125–133.
Xu, X., Zhao, Q., Wuc, M., Ding, J., Zhang, W., 2017. Biodegradation of organic matter and anodic microbial communities analysis in sediment microbial fuel cells with/without Fe(III) oxide addition. Bioresour. Technol. 225, 402–408.
Yu, J., Park, Y., Cho, H., Chun, J., Seon, J., Cho, S., Lee, T., 2012. Variations of electron flux and microbial community in air-cathode microbial fuel cells fed with different substrates. Water Sci. Technol. 66 (4), 748–753.
Yun, Y.M., Lee, M.K., Im, S.W., Marone, A., Trably, E., Shin, S.R., Kim, M.G., Cho, S.K., Kim, D.H., 2018. Biohydrogen production from food waste: current status, limitations, and future perspectives. Bioresour. Technol. 248, 79–87.
Zhang, P., Liu, J., Qu, Y., Feng, Y., 2017. Enhanced *Shewanella oneidensis* MR-1 anode performance by adding fumarate in microbial fuel cell. Chem. Eng. J. 328, 697–702.